# Dimensional crossover and hidden incommensurability in Josephson junction arrays of periodically repeated Sierpinski gaskets

R. Meyer[1], S.E. Korshunov[2], Ch. Leemann[1], and P. Martinoli[1]

[1]*Institut de Physique, Université de Neuchâtel, CH-2000 Neuchâtel, Switzerland*
[2]*L.D. Landau Institute for Theoretical Physics, Kosygina 2, 117940 Moscow, Russia*
(February 1, 2008)

We report a study of overdamped Josephson junction arrays with the geometry of periodically repeated Sierpinski gaskets. These model superconductors share essential geometrical features with truly random (percolative) systems. When exposed to a perpendicular magnetic field $B$, their euclidian or fractal behavior depends on the relation between the intervortex distance (imposed by $B$) and the size of a constituent gasket, and was explored with high-resolution measurements of the sample magnetoinductance $L(B)$. In terms of the frustration parameter $f$ expressing (in units of the superconducting flux quantum) the magnetic flux threading an elementary triangular cell of a gasket, the crossover between the two regimes occurs at $f_{cN} = 1/(2 \times 4^N)$, where $N$ is the gasket order. In the fractal regime ($f > f_{cN}$) a sequence of equally spaced structures corresponding to the set of states with unit cells not larger than a single gasket is observed at multiples of $f_{cN}$, as predicted by theory. The fine structure of $L(f)$ radically changes in the euclidian regime ($f < f_{cN}$), where it is determined by the commensurability of the vortex lattice with the effective potential created by the array. Anomalies observed in both the periodicity and the symmetry of $L(f)$ are attributed to the effect of a hidden incommensurability, which arises from the deformation of the magnetic field distribution caused by the asymmetric diamagnetic response of the superconducting islands forming the arrays.

PACS numbers: 74.80.-g, 74.50.+r, 74.60.Ge, 74.25.Nf

## I. INTRODUCTION

A wide variety of disordered materials, including superconductors, is known to exhibit geometrical inhomogeneities over a broad range of length scales. The properties of such systems can be conveniently described in terms of percolation[1], the simplest idea to understand randomness. Percolation can be regarded as a geometrical phase transition taking place at a "critical concentration" $p_c$ separating a phase of finite clusters ($p < p_c$) from a phase where an infinite cluster is present ($p > p_c$). Like other critical phenomena, it is characterized by a correlation length $\xi_p(p)$ which diverges at the percolation threshold $p_c$. Right at $p_c$, a system with percolative disorder exhibits a natural self-similar structure at all length scales and can therefore be modeled by a family of scale-invariant fractal lattices, such as the Sierpinski gasket (SG), which has been suggested[2] to mimic the essential geometrical features of the percolating cluster's backbone. In the critical region above and below $p_c$, where $\xi_p$ is finite, the nature of the geometry depends on the length scale $l$ at which one is probing the system: if $l < \xi_p$, its structure is *fractal*, whereas it can be regarded as homogeneous with conventional *euclidian* features for $l > \xi_p$.

Allowing an accurate control of both the nature and the amount of disorder and exhibiting properties quite sensitive to dimensionality, Josephson junction arrays and wire networks prepared with modern micro- and nanofabrication techniques provide ideal model systems to investigate the dimensional crossover from the euclid-ian to the fractal regime. The first step in this direction was made by Gordon *et al.*[3], who investigated the superconducting-to-normal phase boundary $T_c(B)$ of aluminum wire networks formed by periodically repeated SGs and of analogous networks with percolative geometry exposed to a perpendicular magnetic field $B$. In those experiments the magnetic length, $l(B) \approx (\phi_0/B)^{1/2}$, which is a measure of the typical nearest-neighbor distance between the vortices present in the system, was shown to be the relevant length scale to explore the euclidian-fractal (EF) crossover ($\phi_0$ is the superconducting flux quantum). While the scaling behavior of the phase boundary of the SG networks was found to exhibit a crossover from the euclidian to the fractal regime consistent with theoretical predictions[4] based on extensions[5,6] of the Ginzburg-Landau theory and allowing for comparison[7] with the anomalous diffusion exponent, no EF crossover was observed in percolative networks which, surprisingly, were found to behave like a homogeneous system at all length scales $l(B)$ probed in the experiment.

More recently, compelling evidence for the EF crossover in a percolative system emerged from ac conductance measurements[8] performed in zero magnetic field on (unfrustrated) site-diluted Josephson junction arrays with site occupation probabilities $p$ very close to $p_c$. In these experiments the crossover was controlled by the driving angular frequency $\omega$, which determines the ratio of the impedances associated with the two types of links forming the random network. According to Efros and Shklovskii[9], the increase of this ratio with decreasing $\omega$ also leads, if $p$ is sufficiently close to $p_c$, to a crossover
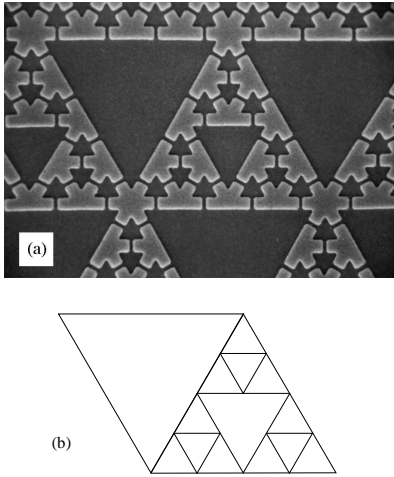
FIG. 1. (a) Scanning electron micrograph showing a portion of a triangular array of periodically repeated second-order Sierpinski gaskets of proximity-effect coupled Pb/Cu/Pb Josephson junctions. The length of the elementary links of the gaskets is $8\mu m$. Notice the "truncated-star" shape of the superconducting Pb islands (with the exception of those centered at the common vertices of three constituent gaskets). (b) The rhombohedral unit cell of a periodic array of second-order gaskets.

from the fractal to the euclidian regime, as confirmed by the experiments of Ref. 8.

In this article we report the results of experimental and theoretical studies of a model superconductor sharing essential geometrical features with a percolative system. The samples we have investigated are arrays of proximity-effect coupled SNS junctions (where S stands for superconductor and N for normal metal) consisting of SGs connected to each other at the vertices in such a way as to form a regular triangular lattice. As can be seen from Fig. 1(a), where a part of an array of second-order gaskets is shown, in these systems the linear size $L_N = 2^N a$ of an individual gasket of order $N$ can be regarded as playing the role of $\xi_p$ ($a$ is the length of an elementary link of the gasket). As shown in detail in this work, a remarkable feature of the SG arrays is that in these systems the EF crossover is clearly manifest, in contrast to truly percolative systems, where its signatures are elusive.

The quantity at the heart of the present study is the magnetoinductance $L(B)$ of the SG arrays, extracted from measurements of their ac impedance. Its interest resides in the observation that, being inversely proportional to the areal superfluid density, it provides a tool to appreciate how the degree of superconducting phase coherence in the system changes with $B$ or, equivalently, with the level of frustration imposed by $B$. Previous impedance measurements performed on weakly frustrated arrays similar to those studied in this work focused merely on the fractal regime and demonstrated, in particular, the unusual scaling properties[10] of the vor-

tex energy[11] as well as the asymptotic $(B \to 0)$ scaling behavior of the field-induced correction to the array inductance resulting from the hierarchical structure of the gaskets[12].

Although some preliminary evidence for a dimensional crossover was already reported in Ref. 12, the phenomenon was not exhaustively investigated. In the present work we rely on high-resolution studies of the complex fine structure of $L(B)$ to explore in detail both the euclidian and the fractal regimes of the SG arrays. Reflecting flux quantization phenomena occurring in loops with a hierarchical distribution of sizes up to the gasket size $L_N$, the fine structure provides a unique tool to reveal how the geometrical properties of the system change as the magnetic length $l(B)$ is swept through $L_N$. We show that, in terms of the frustration parameter $f$ expressing the magnetic flux threading an elementary triangular cell of a gasket in units of $\phi_0$, the EF crossover occurs at $f_{cN} = 1/(2 \times 4^N)$. In the fractal regime ($f > f_{cN}$) the most relevant contributions to the fine structure of $L(f)$ are shown to arise from a particular set of ground states defined by $f = M f_{cN}$, where $M$ is an integer. Corresponding to vortex configurations where the vortex lattice is strongly pinned by the hierarchical potential landscape created by the gaskets, these states are particularly robust against thermal fluctuations and are therefore quite prominent in the fine structure of $L(f)$.

A very interesting aspect emerged from the study of the magnetoinductance in the fractal regime. The analysis of the data revealed anomalous features (specifically, the suppression of the periodicity corresponding to a shift of $f$ by 1 and of the symmetry with respect to $f = 1/2$) inconsistent with theoretical predictions based on the description of the system in terms of a uniformly frustrated $XY$ model. We suggest that, because of the asymmetric shape of the superconducting islands forming the junction pattern of a gasket [see Fig. 1(a)], the screening currents flowing in the islands create a distortion of the magnetic field distribution in the array such that the fluxes threading the various loops slightly deviate from being proportional to their areas. This introduces an effective incommensurability (which we call "hidden" to distinguish it from the "geometric" one studied earlier[13] in wire networks with incommensurate cells) and perturbs the self-similarity of the gaskets. As a result, the system is no longer uniformly frustrated. We demonstrate that the anomalous features mentioned above can be quantitatively accounted for by a simple model, in which the area of the different plaquettes of a gasket is changed according to an appropriate deformation scheme.

Compelling evidence for the existence of the euclidian regime is provided by the array's magnetoinductance for $f < f_{cN}$. Besides the absence of the power-law scaling behavior characteristic of the fractal regime, $L(f)$ contains structures which reflect the presence of ground states corresponding to vortex configurations commensurate with the underlying triangular lattice formed by the largest triangular loops of the array (below $f_{cN}$, it is

energetically unfavorable for vortices to penetrate loops of smaller size), thereby allowing an unambiguous identification of the euclidian regime.

In general, these vortex configurations have the same structure as in the $XY$ model on a honeycomb lattice, but correspond to values of $f$ reduced by a factor of $1/f_{cN} = 2 \times 4^N$. However, the case $f = (1/2)f_{cN}$ requires special attention. In a honeycomb lattice the ground state of the corresponding (fully frustrated) $XY$ model is characterized by an accidental degeneracy, which (to lowest order) survives even in the presence of thermal fluctuations[14]. Owing to the more complex structure of the system, however, this peculiar degeneracy is removed in our SG arrays, allowing to identify the vortex configuration in the ordered phase at $f = (1/2)f_{cN}$.

The paper is organized as follows. Experimental details are given in Sec. II. Sec. III is devoted to the fractal regime ($f > f_{cN}$). Relying on the methods developed in Ref. 12, in Sec. III A we present the calculation of the magnetoinductance of a frustrated SG array for the particular set of frustrations $f = M f_{cN}$ corresponding to the sequence of the most stable states, which are characterized by a relatively compact structure (with a unit cell not larger than a single gasket). Experimental data for the magnetoinductance in the same regime are presented and discussed in Sec. III B, where we show, in particular, how the anomalous features of $L(f)$, revealing the presence of hidden incommensurability, can be accounted for by a simple model, in which the areal changes of different plaquettes (related to the redistribution of the magnetic field) are determined by only one adjustable parameter. In Sec. IV we provide experimental evidence for the existence of the EF crossover and in Sec.V the fine structure of $L(f)$ in the euclidian regime below $f_{cN}$ is shown to be consistent with the existence of vortex states commensurate with the periodic lattice formed by the largest triangular cells of the arrays. A few concluding remarks are given in Sec. VI.

## II. EXPERIMENTAL ASPECTS

The samples studied in this work consist of second-($N = 2$) and fourth-order ($N = 4$) gaskets sitting on the sites of, respectively, a $313 \times 313$ and a $78 \times 78$ triangular lattice and connected to each other at the vertices [see Fig. 1(a)]. Each gasket contains, respectively, $3^{2+1} = 27$ and $3^{4+1} = 243$ SNS Josephson junctions consisting of superconducting Pb islands proximity-effect coupled to each other by an underlying normal Cu layer. The geometrical and physical parameters of the junctions are almost identical to those of the array studied in Ref. 12. Most of the data presented below have been obtained in experiments performed on the array of second-order gaskets.

The sheet magnetoinductance $L(f)$ was inferred from measurements of the array's *linear* sheet impedance $Z =$ $R + i\omega L$ performed with a very sensitive SQUID-operated two-coil mutual inductance technique[15] at driving frequencies typically in the range 0.1-1.0 kHz. With this method we were able to resolve inductance changes of the order of 10 pH in swept-frustration measurements, in which $f$ could be tuned with a precision better than $10^{-3}$. The experimental data are presented and analyzed in terms of $L^{-1}(f)$, the quantity measuring the degree of superconducting phase coherence in the samples. When needed, the resistive component $R(f)$, related to dissipative vortex motion, is also shown for completeness. Additional details concerning the samples and the measuring technique can be found in Ref. 12.

In the following, temperatures are expressed in terms of the reduced temperature relevant for the statistical mechanics of the system, $\tau \equiv k_B T/J(T)$, where $J(T)$ is the temperature-dependent Josephson coupling energy. At temperatures well below the zero-field critical temperature $\tau_{cN}$, $J(T)$ was deduced from measurements of the "bare" sheet kinetic inductance $L(T) = (\phi_0/2\pi)^2(5/3)^N/\sqrt{3}J(T)$ of the unfrustrated samples[12]. Extrapolation to higher temperatures was then achieved by fitting the low-temperature data to theoretical expressions[16] for $J(T)$.

Because of their two-dimensional (2D) nature at length scales larger than $L_N$, both samples are expected to exhibit, at zero frustration ($f = 0$) and in the limit $\omega \to 0$, a Berezinskii-Kosterlitz-Thouless (BKT) phase transition[17]. A sharp depression of $L^{-1}(0)$, which can be associated with the BKT transition, has been indeed observed at, respectively, $\tau_{c2} \approx 0.57$ and $\tau_{c4} \approx 0.23$, in good agreement with the theoretical prediction[10] $\tau_{cN} = (3/5)^N \tau_{c0}$, where $\tau_{c0} \approx 1.5$ is the reduced temperature of the BKT transition of a regular triangular Josephson junction array[18] with the same $J(T)$.

## III. THE FRACTAL REGIME

### A. The ground states of a regular array of Sierpinski gaskets and their sheet inductance

We start by recalling that, within the framework of an approximation ignoring thermal fluctuations, a Josephson junction array behaves, with respect to an external (dc) current source, like a network of inductors $\{L_{ij}\}$, whose inductances are given[12,19] by:

$$L_{ij}(\theta_{ij}) = \frac{(\phi_0/2\pi)^2}{J \cos \theta_{ij}} \quad , \tag{1}$$

where $\theta_{ij}$ is the gauge-invariant phase difference across the link $ij$. As required by fluxoid quantization, the sum of $\theta_{ij}$ around a lattice cell is equal to $2\pi(fS - m)$, where $f$ is the frustration parameter expressing the magnetic flux (in units of $\phi_0$) threading an elementary triangular cell of a gasket [$f = Ba^2\sqrt{3}/(4\phi_0)$], $S$ the area of the cell

(expressed in units of the area of an elementary triangular loop) and $m$ the number of flux quanta (vortices) penetrating the cell under consideration.

In writing Eq. (1) we have assumed that the proximity-effect coupled SNS junctions forming the arrays studied in this work have a sinusoidal current-phase relation at the temperatures of interest[20]. It clearly follows from Eq. (1) that, even if all the junctions are identical, their effective inductances in a frustrated system may differ substantially from each other on account of the nonuniform distribution of $\{\theta_{ij}\}$. Since the array magnetoinductance $L(f)$ can be found by applying Kirchhoff's laws to the inductor network $\{L_{ij}\}$, it is evident that, at any frustration $f$, $L(f)$ will be completely determined once the distribution of $\{\theta_{ij}\}$ is known.

The ground state of a uniformly frustrated array of periodically repeated gaskets of order $N$ [see Fig. 1(a)] can be constructed by a simple juxtaposition after finding the ground state of an isolated $N$th-order gasket only if the constraints of fluxoid quantization imposed on the largest triangular loops (located between the $N$th-order gaskets) are automatically fulfilled. Recalling the definition of $f$ given above, it can be shown[12] that this condition is satisfied only for a particular set of frustrations given by:

$$f = \frac{M}{2 \times 4^N} \qquad , \qquad (2)$$

where $M$ is an integer corresponding to the total number of vortices in the rhombohedral unit cell of the SG array composed, as shown in Fig. 1(b), by a single $N$th-order gasket and the adjacent "empty" triangular loop. Thus, in order to calculate the magnetoinductance of the system at the values of $f$ given by Eq. (2), all we need is to determine the ground-state distribution of $\{\theta_{ij}\}$ in one of its constituent gaskets.

Assuming that the ground state of a gasket is the one having the highest possible symmetry consistent with its reflection and third-order rotation symmetries[21] (for wire networks with the geometry of a third-order SG this conjecture has been confirmed by numerical calculations[22]), it can be shown[23] that the number of independent bond variables $\{\theta_{ij}\}$ is equal to $(3^N+1)/2$. They can be found from an equal number of constraints imposed by current conservation at the nodes and fluxoid quantization in the loops of the gasket. For example, in the second-order gasket of Fig. 2 the links sharing the same symbol have the same values of $\theta_{ij}$, thereby showing that there are only 5 independent bond variables.

Imposing current conservation at one of the 6 equivalent nodes (denoted by $K$ in Fig. 2) and fluxoid quantization in the 4 non-equivalent loops $a$, $b$, $c$, and $d$ (with, respectively, vortex occupation numbers $m_a$, $m_b$, $m_c$, and $m_d$) leads to a system of 5 equations (only one of which, describing current conservation, is nonlinear) which have to be solved numerically under the constraint that the distribution of the quantum numbers $\{m_\alpha\}$ ($\alpha = a, b, c, d$) is such that the gasket energy:
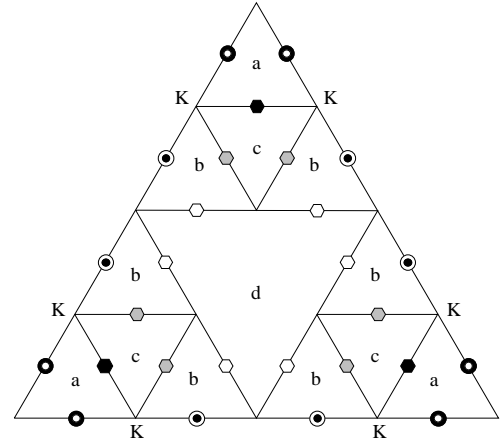


FIG. 2. The links of this second-order gasket sharing the same symbol have identical gauge-invariant phase differences $\theta_{ij}$ in the states whose symmetry is consistent with the reflection and third-order rotation symmetries of the gasket. The 5 independent $\{\theta_{ij}\}$ follow by imposing current conservation at one of the 6 equivalent nodes $K$ and fluxoid quantization in the 4 non-equivalent loops $a$, $b$, $c$ and $d$.

$$E = J \sum_{<ij>} (1 - \cos \theta_{ij}) \qquad (3)$$

is minimized. Quite remarkably, for a given frustration satisfying Eq. (2), the distribution of $\{m_\alpha\}$ corresponding to the lowest energy turns out to be identical[23] to that emerging from a calculation based on junctions with a linear current-phase relation, for which a fully analytical treatment is possible[21,22]. The result is illustrated in Fig. 3, where the ground-state vortex configurations for the rhombohedral unit cell of a regular array of second-order gaskets are shown for $M$ in the range $[0, 40]$.

Inspection of Fig. 3 reveals characteristic features, which are valid for arbitrary gasket order. One first observes that, with increasing frustration, vortex nucleation spreads from the largest to smallest loops[11,22], a property reflecting the hierarchical character of the energy needed to create a vortex excitation[10,11]. Next, one notices that the vortices penetrate the gaskets only for $M > 1$, thereby implying that a SG array will exhibit fractal behavior only for $f > 1/(2 \times 4^N)$. One further recognizes that, since for $M = 1$ the rhombohedral unit cell contains just one single vortex sitting in the largest triangular loop, the ground state of the array at $f = 1/(2 \times 4^N)$ corresponds to a triangular lattice of vortices with a nearest-neighbor distance equal to the gasket size $L_N$. Recalling that $L_N$ plays the role of $\xi_p$, one expects that for $f < 1/(2 \times 4^N)$ the system will behave like a regular Josephson junction array with conventional euclidian geometry. Thus, we identify

$$f_{cN} = \frac{1}{2 \times 4^N} \qquad (4)$$

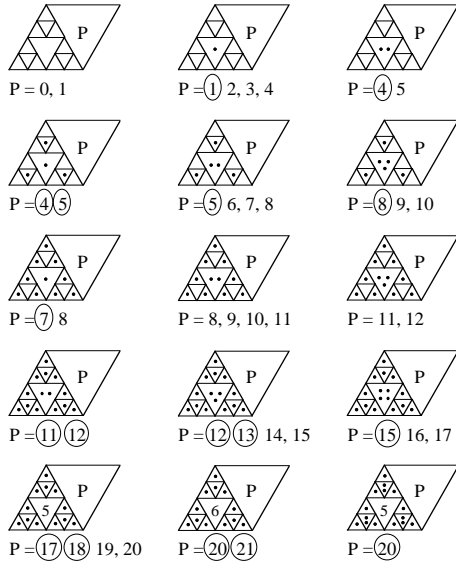as the frustration at which the EF crossover occurs. The

FIG. 3. Ground-state vortex configurations at multiples of $f = 1/32$ in the range $[0, 40]$ for the rhombohedral unit cell of a uniformly frustrated periodic array of (undistorted) second-order gaskets. $P$ denotes the number of vortices in the largest triangular loop. Vortex configurations with circled vortex occupation number $P$ are no longer ground states of the weakly distorted gasket of Fig. 6(a) (see Fig. 7 for a comparison).
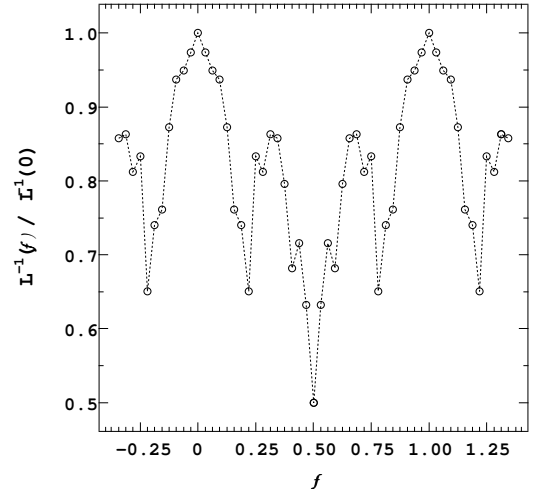


FIG. 4. Normalized inverse magnetoinductance at multiples of $f = 1/32$ in the range $[-11, 43]$ of a uniformly frustrated regular array of (undistorted) second-order gaskets. Notice the symmetry with respect to $f = 1/2$ and the periodicity of period $f = 1$. The dotted line is simply a guide to the eye.

nature of the ground states of the SG array in the euclidian regime $(0 < f < f_{cN})$ is discussed in Sec. V.

Having shown how the structure of the ground state can be determined for the particular set of frustrations (2), we can now proceed with the calculation of the *sheet* magnetoinductance $L(f)$ of the SG array, the quantity measured in our experiments. We first notice that, for this particular set of frustrations, $L(f)$ is proportional to the magnetoinductance of a constituent gasket. Therefore, if we calculate the inductance of a single gasket and normalize it to its value at $f = 0$ to eliminate the trivial dependence on the gasket size, we obtain a result also expressing the normalized sheet magnetoinductance $L(f)/L(0)$ of the composite periodic system. In Ref. 12 we have pointed out that for a given distribution of $\{\theta_{ij}\}$ the calculation of the inductance of a single gasket can be performed by successive application of the triangle-star transformation well known in the theory of electric networks[24]. The result of such a calculation for a regular array of second-order gaskets is shown in Fig. 4 for multiples of $f = 1/32$ in the range $[-11, 43]$. In order to compare this calculation with the experimental data presented in the following subsection, we plot the normalized inverse magnetoinductance $L^{-1}(f)/L^{-1}(0)$. Notice that, as expected for a uniformly frustrated Josephson junction array, $L^{-1}(f)$ is symmetric with respect to $f = 1/2$ and periodic with period $f = 1$. We also recall that, although hardly visible in the linear plot of Fig. 4, in the fractal regime the frustration-induced correction

$\Delta L(f) = L(f) - L(0)$ to the array inductance is predicted to scale[12], in the limit of small frustrations and low temperatures, as $f^\nu$ with $\nu = \ln(125/33)/\ln 4 \approx 0.96$. Obviously, the power-law behavior of $\Delta L(f)$ should no longer persist in the euclidian regime below $f_{cN}$.

So far we have considered only the frustrations given by Eq. (2), for which the ground state of a regular array of gaskets can be regarded as a periodic replication of the ground state of a single gasket. In order to determine the array ground state at rational frustrations differing from those given by Eq. (2), one should consider a "supercell" comprising more than one gasket. The analysis of the ground states based on such supercells rapidly becomes cumbersome and (for $f > f_{cN}$) is not pursued in this work. However, as supercells imply that superconducting phase coherence extends at larger length scales, one can expect the corresponding ground states to be more vulnerable to thermal fluctuations [and, consequently, less prominent in the fine structure of $L(f)$] than those at $f = M f_{cN}$. At these particular values of frustration the vortex configurations (shown in Fig. 3) are strongly pinned by the hierarchical potential landscape provided by the gaskets[11], thereby making these ground states particularly robust against thermal fluctuations.

### B. Comparison with experiment and effects of hidden incommensurability

Focusing on the fine structure of $L(f)$ we now compare the theoretical predictions of Sec. III A with high-resolution magnetoinductance measurements performed on the array of second-order gaskets. Fig. 5(a) shows the normalized inverse sheet magnetoinduc-

tance $L^{-1}(f)/L^{-1}(0)$ of the array of second-order gaskets (measured at 1 kHz) at three different (reduced) temperatures. We first observe that, although the overall shape of the magnetoinductance curves looks roughly similar, the fine structure becomes richer and much sharper with increasing temperature, thereby revealing very clearly almost all the "superfluid" peaks corresponding to the states with a unit cell not larger than a single gasket and belonging to the sequence $f = M/32$ given by Eq. (2). Notice that, to make the identification of the structures easier, the frustration unit on the horizontal axis of Fig. 5(a) is chosen to be equal to $f_{cN} = 1/32$. The striking evolution of the fine structure with temperature suggests that the motion of vortices due to thermal fluctuations plays a major role in the dynamic response of these arrays. We interpret the behavior shown in Fig. 5(a) as clear evidence that, at sufficiently high temperatures, superconducting phase coherence in the neighborhood of the ground states at $f = M/32$, for which the vortex lattice is pinned, is drastically disrupted by vortex-lattice defects, created by excess or missing vortices, moving almost freely on the "frozen" vortex background. This process dramatically sharpens the fine structure, thereby enhancing the amplitude of the oscillations. Similar behavior was also observed in experiments performed on wire networks of interconnected gaskets[11] and in regular triangular Josephson junction arrays[25] as well as in numerical simulations[19].

In sharp contrast to the theoretical prediction for a uniformly frustrated SG array (see Fig. 4), the $L^{-1}(f)/L^{-1}(0)$ curves of Fig. 5(a), although still symmetric with respect to $f = 0$, are no longer periodic with period 1, a behavior leading unavoidably to the suppression of the symmetry with respect to $f = 1/2$. We attribute these anomalous features to the *inhomogeneous frustration* resulting from the change in the effective areas of different plaquettes caused by the asymmetric (with respect to the direction of the links) diamagnetic response of the truncated-star-shaped superconducting (Pb) islands [see Fig. 1(a)]. Because of this particular geometrical form, the screening currents flowing in these grains create a distortion of the current patterns associated with the individual loops which leads to a redistribution of the magnetic field and perturbs the self-similarity of the gaskets. In the temperature range ($5.5K < T < 6.4K$) of the data shown in Fig. 5(a), the magnetic penetration depth of the Pb islands [as estimated from the zero-temperature bulk Pb value ($\lambda(0) \approx 40nm$) and the (proximity-effect reduced) transition temperature ($T_c = 6.9K$) of the Pb grains] is at least 25 times smaller than their smallest planar geometrical dimension, which corresponds to the width of the junctions ($\simeq 2\mu m$). Thus, one expects the distortion of the current patterns and, consequently, the nonuniformity of the frustration to have a considerable effect on $L^{-1}(f)$.

The origin of the phenomenon being intimately related to the geometry of the superconducting islands rather than to the physical properties of the junctions, it seems
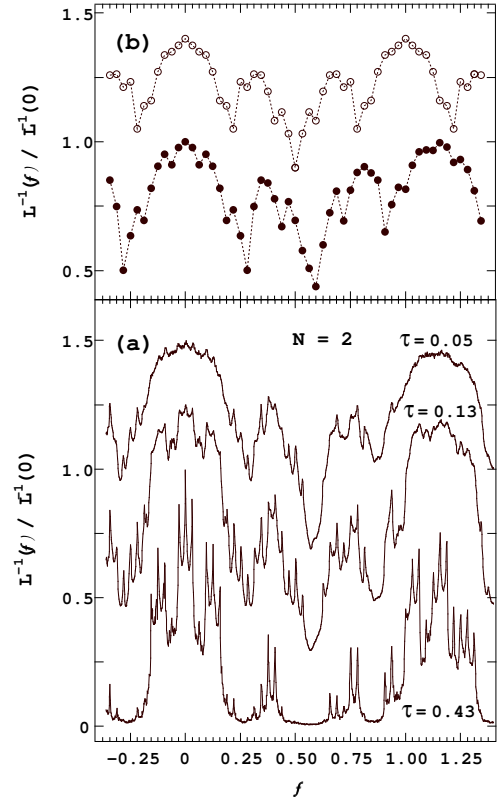


FIG. 5. (a) Normalized inverse magnetoinductance of the periodic array of second-order gaskets shown in Fig. 1(a) measured at 1 kHz at three different temperatures as a function of frustration. For clarity, the curves for $\tau = 0.13$ and $\tau = 0.05$ are shifted upwards by, respectively, 0.25 and 0.50. Notice the absence of periodicity of period 1 and of the related symmetry with respect to $f = 1/2$. (b) Solid circles: normalized inverse magnetoinductance calculated for an array of second-order gaskets deformed as shown in Fig. 6 with $\epsilon = 7.4\%$. This curve should be compared with the data at the lowest temperature ($\tau = 0.05$) in (a). For comparison, the calculation of Fig. 4 for an undistorted SG array is also shown (open circles, the curve is shifted upwards by 0.4 for clarity). The dotted lines in (b) are simply guides to the eye.

plausible to describe the effect of the inhomogeneous frustration by changing merely the effective area of the different plaquettes according to a prescribed rule. This is illustrated in Fig. 6(a) for a second-order gasket, whose distortion is modeled by shifting the vertices of the triangular loops toward the "centers of mass" of the corresponding superconducting islands, as shown in Fig. 6(b). Since the distribution of the screening currents in the islands is shifted in the same direction, this deformation scheme appears to be a reasonable approach offering, above all, the advantage of a simple description in terms of a single paramater, the (small) areal change $\epsilon$ (expressed in units of the area of an elementary triangular cell) defined in Fig. 6(a). Notice, incidentally, that this procedure does not alter the frustrations [Eq. (2)] for which the ground state of the array can be constructed
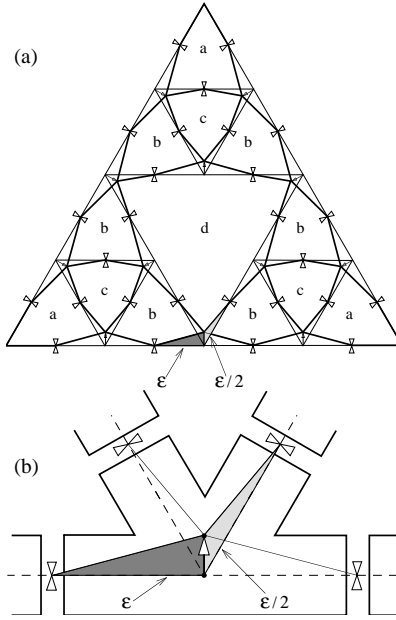
FIG. 6. (a) The deformation scheme (here illustrated for a second-order gasket) introduced to describe the effect of the nonuniform frustration resulting from the distortion of the screening current pattern created by the asymmetric shape of the superconducting islands. The vertices of the triangular loops are shifted towards the "centers of mass" of the corresponding superconducting grains as shown in (b). The areal changes of the loops $a$, $b$, $c$ and $d$ are expressed in terms of the deformation parameter $\epsilon$ (measured in units of the area of an elementary triangular cell) defined in (b).
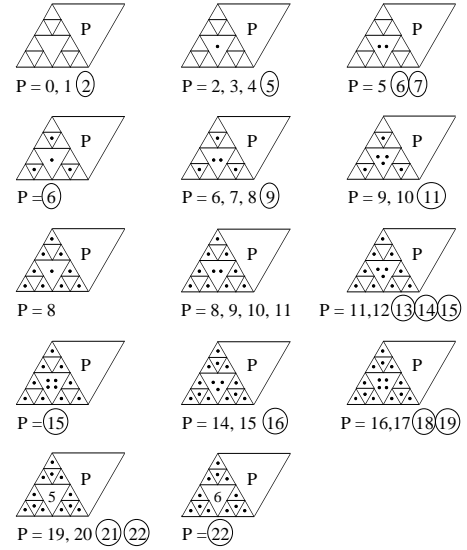


FIG. 7. Ground-state vortex configurations at multiples of $f = 1/32$ in the range $[0, 40]$ for the rhombohedral unit cell of a periodic array of second-order gaskets deformed as shown in Fig. 6(a) with $\epsilon = 7.4\%$. $P$ denotes the number of vortices in the largest triangular loop. The comparison with the ground states of an array of undistorted gaskets of the same order (Fig. 3) reveals that the vortex configurations with circled vortex occupation number $P$ are new ground states of the system.

by a simple juxtaposition of independent gaskets.

As the resulting deformation preserves the reflection and third-order rotation symmetries of the gasket [see Fig. 6(a)], the determination of the vortex and $\{\theta_{ij}\}$ configurations in the highly symmetric ground states at $f = M f_{cN}$ can be carried out by following again the procedure described in Sec. III A. The only modification appears in the formulation of the fluxoid-quantization constraints for the deformed loops, whose areas (and, therefore, the associated magnetic fluxes) change. For example, for the second-order gasket of Fig. 6(a) the areas of the deformed plaquettes $a$, $b$, $c$, and $d$ are equal, in an approximation linear in $\epsilon$, to $1 - \epsilon$, $1 - (3/2)\epsilon$, $1 - 3\epsilon$, and $4 + 3\epsilon$, respectively. An analogous problem, however with a quite different deformation scheme, was considered by Ceccatto et al.[22] for a system with a linear current-phase relation.

Ground-state vortex configurations for the rhombohedral unit cell of an array of second-order gaskets with a deformation parameter $\epsilon = 7.4\%$ (the reason for the choice of this value is explained below) are shown in Fig. 7 for $M$ in the range $[0, 40]$. A comparison with Fig. 3 reveals that some of the ground states of the undistorted array have been replaced by new ones. More precisely, while for the regular SG lattice the symmetry with re-

spect to $f = 1/2$ implies that the ground state for $(1 - f)$ may be conceived as resulting from the superposition of the ground states for $f = 1$ and $-f$, for the distorted system this property no longer holds. The absence of periodicity (corresponding to the $f \leftrightarrow 1 + f$ symmetry) and of the related $f \leftrightarrow 1 - f$ symmetry are clearly reflected in the normalized inverse magnetoinductance shown in Fig. 5(b). This $L^{-1}(f)/L^{-1}(0)$ curve was calculated for an array of second-order gaskets using the method outlined in Sec. III A and was fitted to the low-temperature ($\tau = 0.05$) data of Fig. 5(a) using $\epsilon$ as an adjustable parameter. The best fit was obtained for $\epsilon = 7.4\%$. In this connection, it should be noticed that, although weak, thermal fluctuations still affect the data at $\tau = 0.05$ and tend to enhance the amplitude of the oscillations with respect to that predicted by our calculation, which neglects thermal fluctuations. Nevertheless, the agreement is quite remarkable, especially if one considers that it involves only one fitting parameter. Moreover, the vertex displacement [denoted by the arrow in Fig. 6(b)] defining $\epsilon$ turns out to be $\sim 70\%$ of the distance to the "center of mass" of the truncated-star-shaped superconducting islands, thereby demonstrating the basic validity of our interpretation.

Similar behavior was observed in the magnetoinductance of the array of fourth-order gaskets, whose fine structure was found to be richer than that of the array of second-order gaskets, as demonstrated by the incipient splitting of some of the structures at $f = M/32$.

However, because of the strong overlap resulting from the nonvanishing width of the superfluid peaks, only a fraction of the states at multiples of $f = 1/512$ could be resolved and unambiguously identified in a plot at (relatively) low frustration resolution like that of Fig. 5 (for high-resolution data at very small $f$, see Fig. 9 in Sec. V).

Before closing this section, we would like to notice that when $\epsilon$ is a rational number, the periodicity of $L^{-1}(f)$ is restored, however with a period larger than 1.

## IV. THE CROSSOVER BETWEEN THE TWO REGIMES

Below $f_{cN}$ [see Eq. (4)] the SG arrays are expected to be in the euclidian (or homogeneous) regime. In order to provide preliminary evidence for the existence of the EF crossover at $f_{cN}$, in Fig. 8 we compare, in a log-log plot, the quantity $\Delta L^{-1}(f)/L^{-1}(0) \equiv [L^{-1}(0) - L^{-1}(f)]/L^{-1}(0)$, which measures the relative change in superfluid density caused by frustration, for the two SG arrays studied in this work. Both curves were taken at 160 Hz and at temperatures such that the structures corresponding to the ordered states are emphasized by thermal fluctuations. With decreasing frustration the data for the sample of fourth-order gaskets exhibit, down to $f_{c4} = 1/512$, clear fractal features: specifically, four self-similar stages (the number of stages being consistent with the order of the gaskets) reflecting the dilational symmetry of the gaskets and an overall scaling with $f$ which, in spite of the indisputable evidence for fluctuation effects, follows the asymptotic prediction $\Delta L^{-1}(f) \propto f^{\nu}$. For comparison, the result of a calculation for an undistorted infinite gasket based on the methods discussed in Sec. III A is also shown in Fig. 8. Below $f_{c4}$ the data tend to flatten out, thereby signaling a possible change of regime. However, considering the fact that this change sets in almost at the limit of our inductance resolution ($\Delta L/L \sim 1\%$), we refrain from drawing a firm conclusion with regard to the existence of a dimensional crossover in the array of fourth-order gaskets.

On this subject, the data for the array of second-order gaskets convey a much stronger message. In Sec. III B the magnetoinductance of this sample was shown to obey the predictions for the fractal regime whose signatures, although less pronounced than in the $N = 4$ case, can also be identified, above $f_{c2} = 1/32$, in the log-log plot of Fig. 8 [notice that the self-similar and scaling properties of $\Delta L^{-1}$ are expected to become clearly manifest only in the asymptotic limit ($f \to 0$) of higher-order gaskets[12]. Below $f_{c2}$, however, the behavior of $\Delta L^{-1}(f)/L^{-1}(0)$ drastically changes. Besides the loss of self-similarity and scaling, the data reveal, by closer inspection, the presence of structures [the "dips" in $\Delta L^{-1}(f)$] corresponding to new commensurate states, which can not be ascribed to the fractal regime.
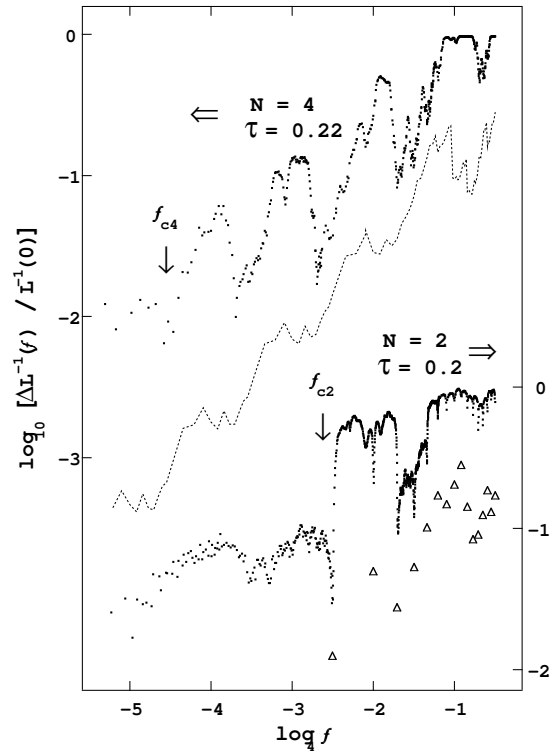


FIG. 8. Log-log plot of the frustration-induced relative change of the inverse sheet inductance of the arrays of second-order ($N = 2$) and fourth-order ($N = 4$) gaskets measured at 160 Hz. The dotted curve is the theoretical prediction for an undistorted gasket of infinite order (see Ref. 12). The result [the same as in Fig. 5(b)] of the calculation for an array of distorted second-order gaskets is shown (open triangles) at multiples of $f = 1/32$ in the range [1, 16]. For clarity, the theoretical curves are shifted downwards by a quarter of a decade. $f_{cN}$ is the frustration at which the crossover from the euclidian ($f < f_{cN}$) to the fractal ($f > f_{cN}$) regime occurs.

To strengthen the evidence for a regime crossover, in Fig. 9 we present the results of sheet inductance measurements performed at high frustration resolution in the range $|f| \leq f_{c2}$. Once again, to promote structures corresponding to ordered states we tuned the effect of thermal fluctuations by increasing the temperature and reducing the measuring frequency (10 Hz) in an appropriate way. Moreover, in Fig. 9 we also include the dissipative component $R(f)$, whose remarkably well resolved fine structure provides additional evidence for the EF crossover. Notice that maxima in the (normalized) superfluid density, $L^{-1}(f)/L^{-1}(0)$, correspond to minima in $R(f)$, as it should be. For the array of fourth-order gaskets both the superfluid and the dissipative components display clear fractal features with marked structures at multiples of $f_{c4} = 1/512$ corresponding to the frustration unit on the $f$-axis. In sharp contrast with this behavior, the dynamic response of the array of second-order gaskets is, within experimental accuracy, symmetric with respect to $f = (1/2)f_{c2}$ and contains well resolved structures
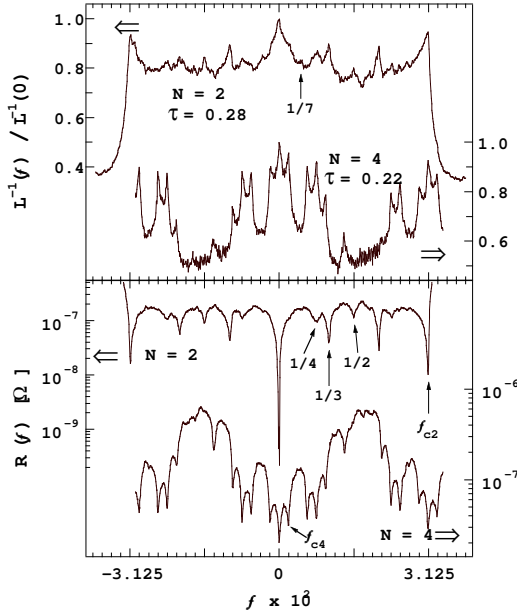
FIG. 9. Normalized inverse magnetoinductance and magnetoresistance of the periodic arrays of second-order ($N = 2$) and fourth-order ($N = 4$) gaskets measured at 10 Hz in the frustration range $|f| \leq f_{c2} = 1/32 = 0.03125$. Structures in the data for $N = 2$ are labeled in terms of $f_H = f/f_{c2}$, the frustration parameter referred to the hexagonal unit cell of the honeycomb lattice shown in Fig. 10. Structures at multiples of $f_{c4} = 1/512$ demonstrate the fractal character of the response for $N = 4$, whereas the prominent structures at $|f_H| = 1/3$ and the symmetry with respect to $f_H = 1/2$ of the data for $N = 2$ are signatures of the euclidian regime.

at $|f| = (1/4)f_{c2}$, $|f| = (1/3)f_{c2}$ and $|f| = (1/2)f_{c2}$. In particular, the presence of prominent structures at $|f| = (1/3)f_{c2}$ provides compelling evidence for the existence of a new regime, since no commensurate state corresponding to this frustration can ever emerge from the characteristic sequence $f = M f_{cN}$ of the fractal regime for gaskets of any order. We interpret these features as an unambiguous signature of the euclidian regime, in which the fine structure of the array's impedance reflects, as shown in the following section, the existence of vortex ground states with a unit cell larger than a second-order gasket.

## V. THE EUCLIDIAN REGIME

In order to understand how our arrays of gaskets behave in the euclidian regime, we first recall that the energy of a vortex in a Sierpinski gasket decreases with increasing size of the cell in which the vortex core is localized[10,11]. Accordingly, a single vortex in a lattice of periodically repeated SGs can be considered as interacting with an external potential whose minima coincide with the centers of the largest triangular cells located between the $N$th-order gaskets and, therefore, form a
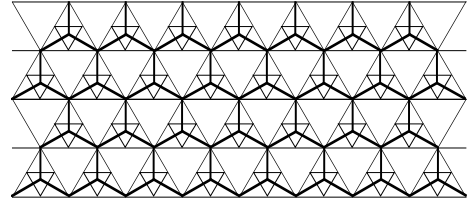


FIG. 10. Successive applications of the triangle-star transformation allow to replace each gasket by an elementary "star", thereby turning a lattice of periodically repeated gaskets into a honeycomb lattice.

triangular lattice. For $f < f_{cN}$ the number of vortices in the system is smaller than the number of the largest triangular cells, so that it is energetically favorable for the vortices to occupy only these largest cells, the concentration of the occupied ones being equal to the ratio $f/f_{cN}$. Therefore, one can expect that, for $f < f_{cN}$, the behavior of an array of periodically repeated SGs resembles that of a uniformly frustrated $XY$-model on a *honeycomb* lattice (with a reduced value of frustration $f_H = f/f_{cN} < 1$), whose ground states can also be thought of as formed by vortices occupying the sites of a triangular lattice with the same concentration $f_H$.

Another approach leading to the same conclusion relies on the iterative procedure, based on successive applications of the triangle-star transformation[24], developed in Ref. 12. At low frustrations, such that there are no vortices in the gaskets, this method allows to replace each gasket by an elementary "star" consisting of three links with a modified interaction. This transforms a lattice of periodically repeated SGs into a honeycomb lattice (see Fig. 10). The difference with respect to the conventional $XY$-model on a honeycomb lattice is that in the iteration process the interaction becomes almost harmonic[12], the anharmonic corrections becoming smaller and smaller as the number of iterations, which is set by the gasket order $N$, increases. Moreover, for $f \neq 0$ the resulting effective interaction is no longer an even function of $\theta_{ij}$[12].

After establishing that the ground states in the euclidian regime ($f < f_{cN}$) are formed by vortices occupying the sites of a triangular lattice with concentration $f_H = f/f_{cN} < 1$, it is natural to expect that the states which are particularly robust against thermal fluctuations correspond to values of $f_H$ allowing the formation of an undistorted triangular vortex lattice (analogous to the Abrikosov lattice in bulk superconductors) commensurate with the underlying lattice provided by the array. The energy required to create a defect in these highly symmetric states is larger than for frustrations requiring the vortex lattice to be distorted. Therefore, these Abrikosov-like states will be less vulnerable to thermal fluctuations. For $1/2 < f_H < 1$ almost equally stable states can be constructed when the vacancies in the densely packed triangular vortex lattice corresponding to $f_H = 1$ also form an undistorted triangular lattice. This leads to the symmetry $f_H \leftrightarrow 1 - f_H$, although it is not

(a) : $f_H = 1/3$    (b) : $f_H = 1/4$

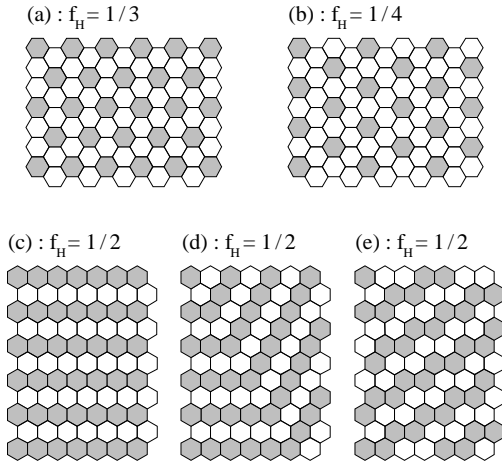(c) : $f_H = 1/2$    (d) : $f_H = 1/2$    (e) : $f_H = 1/2$

FIG. 11. (a) and (b) show ground state Abrikosov-like triangular vortex configurations in a honeycomb lattice at, respectively, $f_H = 1/3$ and $f_H = 1/4$. (c), (d), and (e) are examples of ground-state vortex configurations with the same energy in a honeycomb lattice at $f_H = 1/2$. (c): regular 1D superlattice structure ("striped" phase); (d): a zero-energy domain wall separating two "striped" states of the type shown in (c); (e): the state obtained from (c) by introducing the largest possible number of zero-energy domain walls.

rigorous.

It is readily seen that triangular vortex lattices commensurate with the underlying lattice can be constructed for $f_H = 1/(m^2 + mn + n^2)$, where $m$ and $n$ are integers ($m \geq 1$, $0 \leq n \leq m$). In particular, $m = n = 1$ gives $f_H = 1/3$, $m = 2$ and $n = 0$ give $f_H = 1/4$, $m = 2$ and $n = 1$ give $f_H = 1/7$, etc. The states for $f_H = 1/3$ and $f_H = 1/4$ are shown, respectively, in Figs. 11(a) and 11(b). Within this family, the most "dense" state, i.e. the state for $f_H = 1/3$, can be expected to be, on account of its stronger vortex-vortex interaction, the most stable one, followed, in order of decreasing stability, by those for $f_H = 1/4$ and $f_H = 1/7$. This is precisely what we observe in the magnetoimpedance data of Fig. 9 for the array of second-order gaskets where, focusing on the interval $|f_H| < 1/2$), we find that the most prominent structures, signaling a very stable commensurate state, appear at $|f_H| = 1/3$. Weaker structures corresponding to the next-stable triangular vortex lattice are also well resolved at $|f_H| = 1/4$, whereas structures at $|f_H| = 1/7$ are barely visible and present only in the inverse magnetoinductance data. It is worth mentioning that the observation of the particularly prominent vortex state at $|f_H| = 1/3$ is entirely consistent with theoretical predictions[14,18] as well as with results of Monte Carlo simulations[18] for the frustrated $XY$ model on the honeycomb lattice.

The magnetoimpedance data of Fig. 9 show weak structures also at $|f_H| = 1/2$. The ground states of the $XY$-model on a honeycomb lattice at this particular frustration and the corresponding vortex configurations were studied in Ref. 14 and shown to possess a so-called accidental (i.e., not related to the symmetry) degeneracy, which can be discussed in terms of zero-energy domain walls. Fig. 11(c) shows an example of a ground state for $f_H = 1/2$ characterized by a regular 1D superlattice structure. In this state all the variables $\{\theta_{ij}\}$ take the values $\theta_{ij} = 0, \pm\pi/4$. Redistributing the same set of variables in a different way among the bonds of the lattice allows to transform the state of Fig. 11(c) into another one with the same energy, shown in Fig. 11(d), where a domain wall separates two "striped" states of the type shown in Fig. 11(c). An infinite family of states with the same energy can be constructed by creating sequences of such zero-energy domain walls parallel to each other. Fig. 11(e) shows another example of a periodic ground state, which can be obtained by introducing the largest possible number of domain walls into the state shown in Fig. 11(c).

It is known[26] that in systems allowing the formation of zero-energy domain walls the stabilization of long-range order at nonzero temperatures is achieved if the accidental degeneracy is removed by thermal fluctuations. This mechanism (the so-called "order by disorder"[27]) is relatively weak and, therefore, the ordering in frustrated $XY$-models with accidental degeneracy should be less stable (and destroyed at lower temperatures) than in other $XY$ models. This effect should be even more pronounced for the fully frustrated (i.e. for $f_H = 1/2$) model on a honeycomb lattice, which, in contrast to other 2D $XY$-models with accidental degeneracy[26,28–30], does not display any difference in the spin-wave free energy, calculated in the harmonic approximation, of different periodic ground states[14]. The Monte-Carlo simulations of Shih and Stroud[18] have indeed demonstrated that the phase transition of the frustrated $XY$-model on a honeycomb lattice at $f_H = 1/2$ takes place at a much lower temperature than at $f_H = 1/3$ or $f_H = 1/4$, where the accidental degeneracy is absent.

Returning to the system of periodically repeated SGs at $f = f_{cN}/2$ ($f_H = 1/2$), it is also possible to start the search for its ground state by finding the structure of the state which minimizes the energy (3) for the periodic vortex configuration shown in Fig. 11(c). Obviously, this state is periodic, and its unit cell comprises two gaskets. By redistributing the same set of $\{\theta_{ij}\}$ among the bonds of the lattice in a different way, one can construct the state with the same energy corresponding to the vortex configuration shown in Fig. 11(d). However, in contrast to the fully frustrated $XY$-model on a honeycomb lattice, the state obtained in this way will not be an extremum of the Hamiltonian and, therefore, a slight readjustment of $\{\theta_{ij}\}$ can further decrease its energy. This means that in a system of periodically repeated SGs the domain wall shown in Fig. 11(d) has a negative energy. Accordingly, the state with the lowest energy corresponds to the periodic vortex configuration shown in Fig. 11(e), which is characterized by the highest possible density of such domain walls. The unit cell of this state comprises four

gaskets. In the fully frustrated $XY$-model on a honeycomb lattice a ground state with the same structure is selected if one takes into account the interaction, of arbitrary sign, with the second-nearest neighbors[31].

Thus, the phase transition taking place, with decreasing temperature, at $f_H = 1/2$ should be related to the appearance of long-range order corresponding to the vortex configuration shown in Fig. 11(e). The selection of this state relies on a weak mechanism, which loses its efficiency with increasing $N$, since the effective interaction becomes almost harmonic under decimation. One can therefore expect the ordered phase at $f_H = 1/2$ to be again rather vulnerable to thermal fluctuations. This explains why the structures at $|f_H| = 1/2$ in Fig. 9 are much weaker[32] than those at $|f_H| = 1/3$. Their strength is at most comparable to that of the structures corresponding to the triangular vortex lattice at $f_H = 1/4$, whose weaker vortex-vortex interaction makes the ordering less robust than at $f_H = 1/3$. Numerical simulations[18] show that in the conventional $XY$ model on a honeycomb lattice the ordered phases appear, with decreasing temperature, in the same order: first at $f_H = 1/3$, then at $f_H = 1/4$, and only further down at $f_H = 1/2$.

## VI. CONCLUSION

Our magnetoinductance measurements on Josephson junction arrays of periodically repeated Sierpinski gaskets have clearly demonstrated the existence of two regimes. In agreement with theoretical analysis, in one of them (the fractal regime) the peaks observed in the inverse sheet magnetoinductance, reflecting those states which are the most stable against thermal fluctuations, are equally spaced. Neighboring states in this sequence differ from each other by the penetration of an additional vortex into each unit cell of the array. In the other, euclidian, regime the sequence of the observed stable states corresponds to periodic lattices of vortices occupying the largest triangular cells of the array.

The agreement with theory is achieved not only for the positions of the different peaks, but also for their relative strengths. In the euclidian regime the structure of the ordered states is analogous to that on a honeycomb lattice with reduced frustration and the relative stability of the different states can be understood in terms of vortex lattice disordering. However, the amplitudes of the peaks observed in the fractal regime can be quantitatively explained only if the redistribution of the magnetic field in the array due to the asymmetric shape of the superconducting islands is taken into account. In this connection, we would like to mention the recent work by Park and Huse[33], who compared the energies of different states in a wire network with a *kagomé* lattice geometry at full frustration. These authors came to the conclusion that the effects related to the finite width of the wires can be

compensated by *bending* the wires. This is equivalent to our conjecture that the influence of the asymmetry associated with the screening currents can be reduced to a redistribution of the magnetic field with respect to an ideal system.

The results of our magnitoinductance measurements show that this phenomenon is more pronounced at high frustration levels, an observation consistent with the analysis presented in Sec. III B. Indeed, in our model, the triangular cells exhibiting the largest relative areal changes are the smallest (elementary) ones, which are precisely those providing the dominant contribution to $L^{-1}(f)$ at high values of $f$. Data taken at very small frustrations, like those shown in Fig. 9, are practically unaffected by the nonuniform frustration resulting from the asymmetry of the screening currents.

Early studies[7] of a large-order ($N = 10$) single gasket of superconducting aluminum wires revealed that the period associated with adjacent minima of the superconducting-to-normal phase boundary $T_c(f)$ was larger than that extracted from adjacent maxima. We have found a similar perturbation of the periodic field dependence in our calculations of $L^{-1}(f)$ based on the model for the magnetic field redistribution proposed in Sec. III B. The same mechanism may be responsible for the anomalous feature observed in Ref. 7. It should be noticed, however, that the experiments of Ref. 7 were performed at temperatures very close to $T_c(0)$, where the estimated magnetic penetration depth of the Al wires turns out to be comparable to their width. Accordingly, the effective gasket distortion resulting from screening effects is expected to be weaker than in our arrays. A quantitative verification is therefore needed before drawing a conclusion as for the ability of our model to explain the anomaly observed in Ref. 7.

The influence of the incommensurability of different lattice cells on the magnetoresistance of Josephson junction arrays was discussed by Kosterlitz and Granato[34] in relation to experiments performed on periodic arrays with a complex unit cell[35]. However, quantitative agreement between experiment and theory in treating incommensurability effects in Josephson junction arrays has been demonstrated only by the present work[36]. In our system the phenomenon of incommensurability is present in an hidden form and its manifestations appear as a consequence of the asymmetric shape of the superconducting islands.

[1] For a general review, see, *Fractals and Disordered systems*, edited by A. Bunde and S. Havlin (Springer-Verlag, Berlin, 1991).

[2] Y. Gefen, A. Aharony, B.B. Mandelbrot, and S. Kirkpatrick, Phys. Rev. Lett. **47**, 1771 (1981).

[3] J.M. Gordon, A.M. Goldman, and B. Whitehead, Phys. Rev. Lett. **59**, 2311 (1987); J.M. Gordon and A.M. Goldman, Physica B **152**, 125 (1988).

[4] R. Rammal and G. Toulouse, Phys. Rev. Lett. **49**, 1194 (1982); J.M. Ghez, Y.Y. Wang, R. Rammal, B. Pannetier and J. Bellisard, Sol. State Comm. **64**, 1291 (1987).

[5] P. G. de Gennes, C. R. Acad. Sci. **292**, 9, 279 (1981).

[6] S. Alexander, Phys. Rev. B **27**, 1541 (1983).

[7] J.M. Gordon, A.M. Goldman, J. Maps, D. Costello, R. Tiberio, and B. Whitehead, Phys. Rev. Lett. **56**, 2280 (1986).

[8] A.-L. Eichenberger, J. Affolter, M. Willemin, M. Mombelli, H. Beck, P. Martinoli, and S.E. Korshunov, Phys. Rev. Lett. **77**, 3905 (1996).

[9] A.L. Efros and B.I. Shklovskii, Phys. Status Solidi B **76**, 475 (1976).

[10] A. Vallat, S.E. Korshunov, and H. Beck, Phys. Rev. B **43**, 8482 (1991).

[11] R. Meyer, J.L. Gavilano, B. Jeanneret, R. Théron, Ch. Leemann, H. Beck, and P. Martinoli, Phys. Rev. Lett. **67**, 3022 (1991).

[12] S.E. Korshunov, R. Meyer, and P. Martinoli, Phys. Rev. B **51**, 5914 (1995).

[13] A. Behrooz, M.J. Burns, D. Levine, B. Whitehead, and P.M. Chaikin, Phys. Rev. B **35**, 8396 (1987); P. Santhanam, C.C. Chi, and W.W. Molzen, Phys. Rev. B **37**, 2360 (1988); F. Nori and Q. Niu, Phys. Rev. B **37**, 2364 (1988); Q. Niu and F. Nori, Phys. Rev. B **39**, 2134 (1989).

[14] S.E. Korshunov, J. Stat. Phys. **43**, 17 (1986).

[15] B. Jeanneret, J.L. Gavilano, G.-A. Racine, Ch. Leemann, and P. Martinoli, Appl. Phys. Lett. **55**, 2336 (1989).

[16] A.D. Zaikin and G.F. Zharkov, Sov. J. Low Temp. Phys. **7**, 184 (1981); see also, P. Dubos, H. Courtois, B. Pannetier, F.K. Wilhelm, A.D. Zaikin, and G. Schön, Phys. Rev. B **63**, 064502 (2001).

[17] V.L. Berezinskii, Zh. Eksp. Teor. Fiz. **59**, 907 (1970) [Sov. Phys. - JETP **32**, 493 (1971)]; Zh. Eksp. Teor. Fiz. **61**, 1144 (1971) [Sov. Phys. - JETP **34**, 610 (1972)]; J.M. Kosterlitz and D.J. Thouless, J. Phys. C **5**, L124 (1972); **6**, 1181 (1973); J.M. Kosterlitz, J. Phys. C **7**, 1046 (1974).

[18] W.Y. Shih and D. Stroud, Phys. Rev. B **30**, 6774 (1984); **32**, 158 (1985).

[19] W. Yu and D. Stroud, Phys. Rev. B **50**, 13632 (1994).

[20] K.K. Likharev, Rev. Mod. Phys. **51**, 101 (1979).

[21] S. Alexander and E. Halevi, J. Phys. (Paris) **44**, 805 (1983).

[22] A. Ceccato, S. Doniach, K. Frahm, and B. Mühlschlegel, Z. Phys. B **82**, 257 (1991).

[23] R. Meyer, PhD Thesis, Université de Neuchâtel (1995).

[24] S.B. Senturia and B.D. Wedlock, *Electronic circuits and Applications* (Wiley, New York, 1975), p. 75.

[25] R. Théron, J.-B. Simond, Ch. Leemann, H. Beck, P. Martinoli, and P. Minnhagen, Phys. Rev. Lett. **71**, 1246 (1993).

[26] S. E. Korshunov, A. Vallat and H. Beck, Phys. Rev. B **51**, 3071 (1995).

[27] J. Villain, R. Bidaux, J.P. Carton and R. Conte, J. Phys. (Paris) **41**, 1263 (1980); E.F. Shender, Zh. Eksp. Teor. Fiz. **83**, 326 (1982) [Sov. Phys. - JETP **56**, 178 (1982)].

[28] H. Kawamura, J. Phys. Soc. Jpn. **53**, 2452 (1984); S.E. Korshunov, Pis'ma Zh. Eksp. Teor. Fiz. **41**, 525 (1985) [JETP Lett. **41**, 641 (1985)]; J. Phys. C **19**, 5927 (1986).

[29] C.L. Henley, Phys. Rev. Lett. **62**, 2056 (1989).

[30] G. Franzese, V. Cataudella, S.E. Korshunov and R. Fazio, Phys. Rev. B **62**, R9287 (2000).

[31] S.E. Korshunov (unpublished).

[32] The data **for** $N = 2$ shown in Fig. 9 have been taken at a relatively high temperature $[\tau \approx 0.28 \approx (1/2)\tau_{c2}]$, so that the heights of the peaks are mainly determined by thermal fluctuations.

[33] K. Park and D. Huse, Phys. Rev. B **64**, 134522 (2001).

[34] J.M. Kosterlitz and E. Granato, Phys. Rev. B **34**, 2026 (1986).

[35] R.F. Voss and R.A. Webb, Phys. Rev. B **25**, 3446 (1982); R.A. Webb, R.F. Voss, G. Grinstein and P.M. Horn, Phys. Rev. Lett. **51**, 690 (1983).

[36] Concerning periodic wire networks with incommensurate cells, the agreement between experimental investigations and theoretical calculations of the SN phase boundary $T_c(B)$ was established in Refs. 13.